Hydrogen evolution from a copper(I) oxide photocathode coated with an amorphous molybdenum sulphide catalyst

Carlos G. Morales-Guio[1], S. David Tilley[2], Heron Vrubel[1], Michael Grätzel[2] & Xile Hu[1,*]

[1]Laboratory of Inorganic Synthesis and Catalysis, Institute of Chemical Sciences and Engineering, École Polytechnique Fédérale de Lausanne (EPFL), 1015 Lausanne, Switzerland.

[2]Laboratory of Photonics and Interfaces, Institute of Chemical Sciences and Engineering, École Polytechnique Fédérale de Lausanne (EPFL), 1015 Lausanne, Switzerland.

*Correspondence to: xile.hu@epfl.ch

Abstract

Concerns over climate change resulting from accumulation of anthropogenic CO_2 in the atmosphere and the uncertainty in the amount of recoverable fossil fuel reserves are driving forces for the development of renewable, carbon-neutral energy technologies. A promising clean solution is photoelectrochemical water splitting to produce hydrogen using abundant solar energy. Here we present a simple and scalable technique for the deposition of amorphous molybdenum sulphide films as hydrogen evolution catalyst onto protected copper(I) oxide films. The efficient extraction of excited electrons by the conformal catalyst film leads to photocurrents of up to -5.7 mA cm^{-2} at 0 V versus the reversible hydrogen electrode (pH 1.0) under simulated AM 1.5 solar illumination. Furthermore, the photocathode exhibits enhanced stability under acidic environments, whereas photocathodes with platinum nanoparticles as catalyst deactivate more rapidly under identical conditions. The work demonstrates the potential of earth-abundant light-harvesting material and catalyst for solar hydrogen production.

Among the different sources of renewable energy (solar, wind, geothermal, biomass, hydroelectric, tidal and nuclear), only solar energy can be exploited on a scale commensurate with our growing energy requirements[1]. To be of practical interest, light harvesting must be coupled to efficient energy storage mechanisms in order to keep a constant energy supply during the periods of lower sunlight irradiation or at night. The storage of solar energy in the form of hydrogen is an ideal solution since hydrogen can be produced directly from water and converted back to electricity when needed using a fuel cell[2]. However, in order to collect solar energy on the terawatt scale, these devices need to be made of abundant materials and should ideally reach or exceed 10% solar-to-hydrogen conversion efficiencies.

Photoelectrochemical (PEC) water splitting is attractive as it integrates in the same device both solar energy collection and water electrolysis. Like electrolysers, a PEC water splitting device requires a catalyst for the hydrogen evolution reaction (HER). Ideal HER catalysts for PEC water splitting need not only produce hydrogen at low overpotentials but should also be optically transparent and form a stable electrical contact with the photoabsorbing material[3,4]. Pt, the best HER catalyst, is often deposited on a photocathode to promote PEC hydrogen production[5-10]. Pt is however too scarce and costly for a large scale application. Thus, there is a growing interest to apply earth-abundant and non-precious metal HER catalysts for PEC hydrogen production[11-17].

We have developed amorphous molybdenum sulphide films as HER catalysts under acidic and neutral conditions[18-20]. While the as-prepared precatalysts might have various compositions depending on the synthetic procedure, the active species is the same and is best labeled as MoS_{2+x}[20]. The latter species has a Mo:S ratio close to 1:2, and contain both S_2^{2-} and S^{2-} ligands, with a S_2^{2-}:S^{2-} ratio of about 3:7 according to X-ray photoelectron spectroscopy (XPS)[20]. In this work, we derive a PEC method to deposit amorphous MoS_{2+x} films onto surface-protected cuprous oxide photocathodes. Surface-protected Cu_2O is arguably the state-of-the-art *p*-type oxide for PEC hydrogen production[10] and one of the most promising low-cost materials reported until now[21]. The

direct band gap of Cu_2O is suitable for capturing a large portion of the visible spectrum with a maximum solar-to-hydrogen (STH) efficiency of 18.1% based on the AM 1.5 irradiance spectrum and a corresponding photocurrent of -14.7 mA cm^{-2} (E_g of Cu_2O = 2.0 eV)[10]. The MoS_{2+x} catalyst shows activity comparable to that of previously reported Pt nanoparticles[10,22] and RuO_x[23] deposited on the same surface-protected Cu_2O photocathode. Moreover, compared with Pt, the MoS_{2+x} catalyst gives an improved stability in PEC hydrogen production under acidic conditions.

Results

MoS_{2+x}-Coated Cu_2O Photocathode. The Cu_2O photocathode was prepared by an electrodeposition method similar to a previously reported protocol[22,24]. Detailed description of the experimental method is given in the Methods section. In brief, thin Cu_2O films were deposited electrochemically from a lactate-stabilized copper sulphate plating bath kept at 30^oC in a two-electrode configuration cell at a constant galvanostatic current density of -0.1 mA cm^{-2} for 105 minutes. In this work a freshly polished titanium plate was used instead of a Pt mesh as counter electrode during the device preparation process in order to avoid Pt contamination. Subsequently, ultrathin protective layers of aluminium-doped zinc oxide (AZO, 20 nm) and titanium dioxide (100 nm) were deposited by atomic layer deposition (ALD). The TiO_2 overlayer protects the buried Cu_2O/AZO photovoltaic junction from the aqueous environment and transports the photogenerated electrons to the electrolyte where water reduction takes place[8,22]. Figure 1a is a schematic representation of photolytic HER from this device.

The photoelectrochemical deposition of MoS_{2+x} was carried out utilizing unfiltered irradiation from a Xe lamp. The surface-protected Cu_2O photocathode was immersed in an aqueous solution containing 0.2 mM $(NH_4)_2MoS_4$ and 0.1 M NaClO4 (pH 6.8). The MoS_{2+x} catalyst was deposited following two routes: in the first route, consecutive cyclic voltammograms (typically 160 cycles) were carried out between 0.2 and 1.7 V vs. the reversible hydrogen electrode (RHE) at a scan rate of 0.05 V s^{-1} starting

and ending at the cathodic potential (Supplementary Fig. 1). This photocathode is denoted as MoS_{2+x}-CV-Cu_2O. The second route consisted of an anodic photoelectrodeposition at a constant potential of 1.7 V vs. RHE (MoS_{2+x}-CA-Cu_2O) during 150 min. Figure 1b is a photograph of this photoelectrode. It should be noted that no oxidative deposition occurs when a KG3 IR/UV filter is interposed between the light source and the photoabsorber (inset in Supplementary Fig. 1a). Thus, oxidation processes in the multi-layer photocathode depend on the absorption of short wavelength photons (<380 nm) that generate holes in the TiO_2 overlayer (*vide infra*).

Characterization of the surface-protected Cu_2O before and after deposition of the MoS_{2+x} catalyst indicate the formation of a conformal HER catalyst film (Fig. 2 and Supplementary Fig. 2). The thin Cu_2O films used for this study consist of a thin film of 400 nm finished by surface grains with an average size of 273 nm. Grain size distribution was determined by analysis of SEM images before HER catalyst deposition as shown in the Supplementary Fig. 3. The SEM cross-section image of the MoS_{2+x}-CV-Cu_2O photocathode in Fig. 2c shows a thick layer (~50-100 nm) of MoS_{2+x} deposited on top of the AZO and TiO_2 protective layers. Wide-range XPS analysis of the photocathode surface indicates the presence of mainly Mo and S and the absence of Ti, Cu or Zn further confirming the creation of a conformal film of at least 10 nm thick on top of the layered device (Supplementary Fig. 4). The XPS spectra of the as-prepared molybdenum sulphide catalysts on Cu_2O are similar to those earlier deposited by electrochemical methods on a FTO electrode (Supplementary Fig. 5)[18]. Detailed description of XPS data fitting is given in Supplementary Note 1 and Supplementary Tables 1 and 2. The precatalyst in MoS_{2+x}-CA-Cu_2O resembles MoS_3, whereas that in MoS_{2+x}-CV-Cu_2O films resembles MoS_{2+x}[20]. In agreement with our previous observations for electrocatalytic hydrogen evolution[20], the precatalyst in MoS_{2+x}-CA-Cu_2O is transformed into MoS_{2+x} during photocatalysis (*vide infra*).

PEC hydrogen evolution property. The MoS_{2+x}-Cu_2O photocathodes were tested for hydrogen evolution under simulated AM 1.5 solar illumination. Thorough characterization of the photovoltaic

properties of the surface-protected Cu_2O photocathode utilizing a RuO_x catalyst, including the incident-photon-to-current efficiency (IPCE) and validation of the light source, has been previously reported[23]. Figure 3 displays the current-potential curves in the dark and under illumination for a MoS_{2+x}-CV-Cu_2O photocathode (catalyst loading 30 μg cm^{-2}). A photocurrent of -5.7 mA cm^{-2} at 0 V vs. RHE (i.e., no thermodynamic bias) was obtained at pH = 1. The onset potential of photocurrent is +0.45 V vs. RHE and the dark currents are negligible. Similar currents were obtained for the MoS_{2+x}-CA-Cu_2O photocathode (Supplementary Fig. 6a). The activity of MoS_{2+x} is comparable to Pt and RuO_x deposited on the same photocathode (Supplementary Table 3). The early onset potential is noteworthy and reflects the high photovoltage provided by the Cu_2O/AZO junction. Comparison with a similar Cu_2O photocathode loaded with Pt nanoparticles shows a difference of 150 mV for the onset potential. This is in agreement with the activity of amorphous MoS_{2+x} and Pt for electrochemical hydrogen evolution[18]. Chorkendorff and co-workers also found that the onset potential of a MoS_x catalyst is 145 mV more negative than that of Pt on a Ti-n^+p-Si photoelectrode[13].

Interestingly, the MoS_{2+x} catalyst is active for PEC hydrogen evolution under both acid and slightly basic conditions. From pH = 1.0 to pH = 4.0, and with the same catalyst loading of 30 μg cm^{-2}, only a small decrease in photocurrents was observed. Increasing pH further decreased significantly the photocurrent. Still, a substantial current density of -2.3 mA cm^{-2} could be obtained at pH = 9.0 at 0V vs. RHE. The decrease of photocurrent and worsening of the fill factor at higher pHs is consistent with the electrochemical activity of MoS_{2+x} films grown on FTO (Supplementary Fig. 7)[18]. The photocurrents at high pH, however, can be increased by applying a higher loading of catalyst (Supplementary Fig. 8). At pH = 5.0, a photocurrent of -4.5 mA cm^{-2} was obtained with a MoS_{2+x} loading of 50-70 μg cm^{-2}. At an even higher loading of catalyst, however, the photocurrent decreased, which is likely due to the absorption of light by the MoS_{2+x} film that decreases the irradiation on the Cu_2O electrode[18].

At pH = 1.0 and within the range of 20-50 μg cm^{-2} of MoS_{2+x} loading, the photocurrents are independent of catalyst loading, probably because at this pH the extraction of excited electrons by the HER catalyst is so efficient that it is already maximized at a low loading. The fast electron extraction by the MoS_{2+x} film at pH 1.0 is evident, as the transient behavior is not observed under chopped light illumination at potentials negative of 0.3 V vs. RHE (Supplementary Fig. S6b). Similar to pH = 5.0, the photocurrent decreased when the loading exceeded 50 μg cm^{-2}, again likely due to the absorption of light by the catalyst. The coupling of HER catalysts to semiconductor devices requires a compromise between higher surface area with higher catalyst loadings and the degree of incident light absorbed or reflected by the catalyst[3].

The contributions to the photocurrent due to photon absorption by the TiO_2 protective overlayer and the MoS_{2+x} are negligible under simulated AM 1.5 illumination. As a control experiment, the current behavior under light and in the dark for a dummy photocathode consisting of only a MoS_{2+x} film grown on 100 nm of TiO_2 was measured at 0 V vs. RHE (Supplementary Fig. 9a). The photocurrents are three orders of magnitude smaller than the photocurrents observed under the same conditions for the MoS_{2+x}-CA-Cu_2O and MoS_{2+x}-CV-Cu_2O photocathodes. The spectrum of light reaching the photocathode shown in Supplementary Fig. 9b resembles closely the AM 1.5G solar spectrum where the contribution of wavelengths in the near ultraviolet region that could excite electrons over the TiO_2 bandgap is small.

The preparation of the photocathodes and the performance observed are reproducible and the results shown here correspond to the compilation of data obtained for more than 40 photocathodes prepared in more than 7 different batches during a period of six months. The current densities are independent of the area covered with catalyst and exposed to illumination. The active areas of the photocathodes varied from 0.2 to 0.8 cm^2 without any noticeable difference in performance per unit area.

The photocurrents measured under optimized conditions (-5.7 mA cm^{-2} at 0 V vs. RHE and pH 1.0) are the same as previously reported with the RuO_x catalyst at pH 5[23]. To the best of our knowledge this value is the highest ever reported for a Cu_2O material without the use of noble-metal HER catalysts (Supplementary Table 4). Previous efforts to produce hydrogen from NiO_x-coated *p*-Cu_2O[16] and carbon-protected *p*-Cu_2O[14] photoelectrodes have shown initial photocurrent densities of -4.98 and -3.95 mA cm^{-2}, respectively, at 0V vs. RHE. Although these photocathodes show remarkable initial photocurrent, they quickly deactivate over a period of 20 min and show low Faradaic efficiency (Supplementary Table 4).

Photocathode stability and Faradaic efficiency. Long term photocatalytic hydrogen evolution measurements under simulated AM 1.5 illumination show that the use of MoS_{2+x} as HER catalyst increases the stability of the photocathode (Fig. 4a). At pH = 4.0, the photocurrent is stable at -4.5 mA cm^{-2} for 10 hours under continuous illumination for a MoS_{2+x}-CV-Cu_2O photocathode. The MoS_{2+x}-CV-Cu_2O photocathode is also stable at pH 9.0 and a substantial current density of -2.0 mA cm^{-2} was observed during 10 hours. At pH = 1.0, the photocurrent gradually decreases to below -1 mA cm^{-2} after 7 hours. On the contrary, the photocurrents from a Pt-Cu_2O photocathode are less stable. At pH = 5.0, it was shown earlier that only 62% of the initial photocurrent was conserved after 10 h of testing under chopped light[22]; at pH = 1.0, the current erodes within 3 hours according to the current study (Fig. 4a).

The decrease of the photocurrent of TiO_2-protected Cu_2O photocathodes is normally attributed to three main factors: i) the dissolution of the amorphous TiO_2 by acid; ii) the formation of Ti^{3+} electron traps in the titania film; iii) the detachment of the HER catalyst during photoelectrolysis[8,10]. Whereas Pt islands do not prevent the corrosion of TiO_2, MoS_{2+x} films seem to form a conformal layer that better isolates the inner layers from the solution, reducing the contact between TiO_2 and acid. This is consistent with the cross section SEM images of the MoS_{2+x}-CV-Cu_2O photocathode (Fig. 2c).

Furthermore, amorphous MoS_{2+x} films are stable in strongly acidic conditions[18] and SEM shows that a thin layer of MoS_{2+x} remains on the surface of the photocathodes after 1 h of photolytic HER (Supplementary Figs 2c and 2g). It should be noted that the stability issues of Pt- Cu_2O photocathodes are not due to the lower stability of Pt catalyst, but due to the detachment of Pt nanoparticles from the TiO_2 surface (pH = 5.0)[22], and the dissolution of the TiO_2 layer (pH = 1.0). Photoelectrochemical measurements of protected Cu_2O without a HER catalyst showed that the TiO_2 layer dissolved over time at pH 1.0 while it is stable at pH 4.0 (Supplementary Fig. 10). The deposition of protective layers different from TiO_2 with a higher stability in acid might further improve the stability of the whole device. Recently, Chorkendorff and co-workers demonstrated that MoS_2, a more stable material than TiO_2 in acid, can act as a protective layer when grown directly on n^+p-Si photocathodes[17].

Hydrogen production efficiency of a MoS_{2+x}-CA-Cu_2O photocathode under AM 1.5 illumination was probed at pH 4.0 (Fig. 4b). A stable photocurrent density was obtained under illumination whereas the dark current was negligible at 0 V vs. RHE (Supplementary Fig. 11a). Bulk photoelectrolysis shows a faradaic efficiency close to 100% after a small induction period of 20 min (Figs 4b and Supplementary Fig. 11b). The induction time is associated with the reduction of MoS_3 to the active phase of MoS_{2+x} (see Supplementary Note 1 for detailed XPS characterization) and the dissolution of the initially produced H_2 in the air saturated electrolyte.

Discussion

Mott-Schottky analysis for the different layers of the device was used to determine the flat band potential and estimate the dopant density in the near-surface region (see Supplementary Note 2 and Supplementary Figs 12 and 13). Fig. 5 shows the schematic relative band position for the multijunction photocathode after equilibration in the dark assuming band edge pinning at the interfaces and taking the built-in potentials at the interfaces equal to the difference in Fermi level[22].

The electrochemical potential of the solution is taken as the HER level, which is true under conditions of hydrogen evolution at the photocathode. The band position diagram in Fig. 5 explains many of the characteristic features observed in this device. First, the layered structure cannot drive any oxidative deposition of the HER catalyst in the semiconductor-electrolyte interface in the absence of high energy photons. The high potential barrier at the *n*-AZO and the *p*-Cu_2O interface prevents any electrons from flowing from the TiO_2 to the Cu_2O layer through the valence band. The absorption of high energy photons by the TiO_2 from the unfiltered Xe lamp creates holes that drive oxidative PEC deposition of the MoS_{2+x} catalyst. Photo-excited electrons avoid recombination and flow through the conduction band of the overlayers into the Cu_2O valence band when the photocathode is biased at potentials more positive than the flat band potential of the Cu_2O layer (+0.81 V vs. RHE, Supplementary Table 53) as observed in the inset of Supplementary Fig. 1a and depicted in Supplementary Fig. 14. Second, the conduction band of the *n*-type AZO, TiO_2 and MoS_{2+x} have a position more reductive than the HER potential which is favorable for the conduction of photogenerated electrons in the photocathode as confirmed by this work (Supplementary Fig. 14a). The photovoltage of the buried *p-n* junction has been experimentally found to be between 0.5 and 0.6 V[23]. This explains the onset potential for hydrogen evolution at +0.6 V observed for Pt on this photocathode and +0.45 V for the MoS_{2+x} catalyst.

In summary, we have successfully deposited MoS_{2+x} films as a HER catalyst on TiO_2-protected Cu_2O photocathodes. The catalyst displays many features that are desirable for a PEC water splitting device: simple and scalable process of deposition, optical transparency, stability during 10 h of continuous operation, and low overpotential for the HER. The integrated device produces photocurrents as high as -5.7 mA cm^{-2} at 0V vs. RHE (photocurrents that would correspond to 7% STH efficiency in a tandem cell configuration) with a ~100% Faradaic yield. Moreover, the layered device reported here is the most active Cu_2O photocathode to date that makes use of an earth-abundant HER catalyst (Supplementary Tables 3 and 4).

Methods

All manipulations were carried out under atmospheric conditions, unless otherwise mentioned. All reagents were purchased from commercial sources and used without further purification. Millipore de-ionized water 18.2 MΩ was used to prepare all the solutions.

Cu_2O electrodeposition. The Cu_2O thin films were deposited by electrodeposition from a basic solution of lactate-stabilized copper sulphate as previously reported by one of our groups.[10] In brief, Cu_2O thin films were deposited in a plating bath kept at 30 ^oC using a potentiostat (IviumStat) in a two-electrode configuration cell at a constant current density of -0.1 mA cm^{-2} (Galvanostatic mode) for 105 minutes. The deposition electrode was a 70x30 mm TEC^{TM}-15 fluorine-doped tin oxide (NGS glass) coated with 10 nm Cr and 150 nm of Au (deposited by sputtering) and the counter electrode was a 25x25 mm Ti metal plate. The titanium counter electrode was used in order to avoid any Pt contamination of the device. The plating bath was an aqueous 0.2 M $CuSO_4$ (Sigma Aldrich, 98+%) and 3 M lactic acid (Roth, 90%) solution with 0.5 M K_2HPO_4 (Sigma, 98+%) buffer. The bath pH was adjusted to pH 12 using a 2 M KOH (Reactolab) solution. The plating bath concentrations refer to the initial bath concentration prior to pH adjustment.

Atomic layer deposition ALD. Atomic layer deposition was used to deposit ultrathin layers of n-type oxides on the surface of the Cu_2O thin films using a thermal ALD system (Savannah 100, Cambridge Nanotech). The general conditions for ALD have been optimized and reported by Paracchino *et al.*.[22] Typically, the ALD of Al:ZnO (AZO) was carried out at a substrate temperature of 120 ^0C. The precursors were diethylzinc (ABCR, 95%), trimethyl aluminium (ABCR, 98%) and H_2O kept at room temperature as the Zn, Al and O precursors, respectively. Each precursor was held in the chamber for 2.0 s, followed by a 15 s nitrogen purge. Aluminium-doped ZnO (Al:ZnO) was deposited by intercalating one cycle of trimethyl aluminium and water after 20 cycles of diethyl zinc and water. The growth rate per cycle (GPC) under these conditions was previously determined to be 1.7 Å and

2.0 Å for Al_2O_3 and ZnO, respectively. Titanium dioxide (TiO_2) was deposited at a substrate temperature of 150 ^{0}C using tetrakis-(dimethylamino)titanium, TDMAT (99.99%, Aldrich), at a precursor temperature of 75 ^{0}C, and hydrogen peroxide (50% in water, stabilized, Aldrich) at room temperature. TiO_2 was deposited in pulse mode under a nitrogen flow of 5 sccm, with a pulse length of 0.1 seconds and wait period of 10 seconds for both precursors. The growth per cycle (GPC) for TiO_2 was determined by ellipsometry on a silicon wafer with native oxide and corresponded to 0.58 Å cycle^{-1} at 150 ^{0}C.

MoS_{2+x} HER catalyst photoelectrochemical deposition. The deposition of MoS_{2+x} catalyst on the Cu_2O photocathode coated with AZO and TiO_2 overlayers was done under non filtered irradiation from a 180 W Xe lamp (Osram). The illumination intensity on the deposition cell was 130 mW cm^{-2}. Epoxy resin or Teflon tape was used to cover any Au or FTO substrate exposed and to limit the area of catalyst deposition.

A freshly prepared photocathode was immersed into a 0.2 mM aqueous solution of $(NH_4)_2MoS_4$ (Aldrich, 99.97%) in 0.1 M $NaClO_4$ (ABCR, 99%) at a pH of 6.8. Both chemicals were used as received. The MoS_{2+x} catalyst was deposited following two routes: in the first route, consecutive cyclic voltammograms (typically 160) were carried out on an IviumStat potentiostat (Ivium Technologies) with a saturated Ag/AgCl reference electrode (separated by a porous silica gel frit) and a Ti wire counter electrode. The cyclic voltammograms were performed between 0.2 and 1.7 V vs. RHE at a scan rate of 0.05 V s^{-1} starting and ending at the cathodic potential (photocathode identified as MoS_{2+x}-CV-Cu_2O). The second method consisted of the same conditions as described above, but instead of consecutive voltammograms, a constant potential of 1.7 V vs. RHE was applied for different periods of time (photocathode identified as MoS_{2+x}-CA-Cu_2O). For Mott-Schottky analysis and study of the contribution to the photocurrent from photon absorption by the TiO_2, the same procedure was used to deposit MoS_{2+x} catalyst films on electrodes consisting of a 100 nm TiO_2 layer grown by ALD on FTO.

Pt nanoparticles deposition on surface-protected Cu_2O. Platinum nanoparticles were galvanostatically electrodeposited in the dark from a 1 mM aqueous solution of H_2PtCl_6 (ABCR, 99.9%) (pH = 2.4). A current density of -8.5 μA cm^{-2} was kept during 15 minutes.[22]

Physical and chemical characterization. The electrodes were characterized by SEM and XPS. SEM secondary electron (SE) images were taken on a Philips (FEI) XLF-30 FEG scanning electron microscope. ImageJ software was used to measure the distances in SEM images. X-ray photoelectron spectroscopy (XPS) data were collected on an Axis Ultra instrument (Kratos Analytical) under ultrahigh vacuum (<10^{-8} torr) using a monochromatic Al K_α X-ray source (1486.6 eV), in the Surface Analysis Laboratory of CIME at EPFL. The source power was maintained at 150 W (10 mA, 15 kV). The adventitious carbon 1s peak was calibrated at 284.8 eV and used as an internal standard to compensate for any charging effects. Both curve fitting of the spectra and quantification were carried out with the CasaXPS software, using relative sensitivity factors from the supplier.

PEC Measurements. Photoelectrochemical measurements were recorded by an IviumStat electrochemical analyzer. A three electrode configuration under front-side simulated AM 1.5 illumination was used where a Pt wire was used as the counter electrode and an Ag/AgCl (KCl sat.) electrode was used as the reference electrode. Different electrolyte buffer solutions were used at different pH values and were referenced in the text by the pH value unless otherwise mentioned. pH 5.0 solution consisted of a 1.0 M Na_2SO_4 (Sial, 99+%) buffered with 0.1 M K_3PO_4 (Aldrich, 97%). pH 4.0 solution consisted of 0.5 M Na_2SO_4 with 0.2 M potassium hydrogen phtalate (Fluka, 99.5+%) buffer. Solutions of 0.5 M Na_2SO_4 buffered with 0.1 M formic acid (Merck, 98-100%) and 0.1 M phosphoric acid (ABCR, 98%) were used as pH 3.0 and pH 2.0 buffer solution, respectively. pH 9.0 solution consisted of 0.1 M sodium tetraborate (Sial, 99.5+%). Finally, 0.1 M H_2SO_4 (Merck, 95-97%) was used as pH 1.0 and 0.1 M NaOH (Riedel, 98-100%) was used as pH 12.9 solutions. The photoresponse was measured under irradiation from a 450 W Xe lamp (Osram) equipped with a KG3 filter (3 mm, Schott, filters UV and IR light; see Supplementary Fig. 9b), calibrated with a Si diode to simulate AM 1.5

illumination (100 mW cm^{-2} = 1 sun). The scan rate for the linear sweep voltammetry was 10 mV s^{-1} in the cathodic direction. Photocurrent stability test were carried out by measuring the photocurrent produced under constant light irradiation at a fixed electrode potential of 0 V vs. RHE. During linear sweep voltammetry (*j*-V plots) and chronoamperometry (stability plots) the electrolyte was continuously bubbled with N_2 to remove oxygen and thus eliminate erroneous signals arising from oxygen reduction. The electrochemical impedance spectroscopy (EIS) measurements were carried out using an Autolab potentiostat/galvanostat. Impedance measurements on freshly electrodeposited Cu_2O films were carried out in the dark using a 3-electrode configuration. The electrolyte was 0.1 M sodium acetate (Aldrich, 99+%) (pH 7.85) in water. The potential was swept in the range of stability predicted by the Pourbaix diagram (0.4 - 0.6 V vs. RHE) and an AC signal of 10 mV of amplitude was superposed on the DC component. Before EIS measurements, the electrode was dipped for 15 s in a 0.8 M acetic acid solution to remove the native CuO layer on the surface. EIS measurements for ALD TiO_2 (100 nm) on FTO were carried out in a 0.1 M NaOH (pH 12.9) between 0.5 and 1.0 V vs. RHE. Impedance measurements for MoS_{2+x} on TiO_2 (100 nm) were carried out in the KHP buffer solution (pH 4.0). EIS experimental data was analyzed and fitted using ZView software (Scribner Associates).

Hydrogen measurements were taken in a manner similar to the photocurrent measurements at a constant potential of 0 V vs. RHE under chopped 1 sun AM 1.5 illumination in a H-cell calibrated for hydrogen evolution measurements as described in the literature and adapted with a optically transparent window for light irradiation[25]. The electrolyte used was KHP buffer solution (pH 4.0). The Faradaic efficiency was calculated from the total amount of charge Q(C) passed through the cell and the total amount of hydrogen produced n_{H2} (mol). The total charge was obtained from the integration of the measured current. The total amount of hydrogen produced was measured using a calibrated pressure sensor. For the reduction of protons, two electrons are needed to reduce two protons and produce one H_2 molecule. Thus, the Faradaic efficiency can be calculated using the equation Faradaic efficiency = $n_{H2}/(Q/2F)$, where *F* is the Faraday constant.

Stability tests were carried out in a manner similar to the photocurrent measurements at a constant potential of 0 V vs. RHE with constant nitrogen overflow.

Light source spectra determination. Light source spectra were obtained using an Ocean Optics USB2000+ Fiber Optic Spectrometer (responsive from 200 to 1100 nm) with SpectraSuite software. The irradiance of the light source with and without the KG3 filter was measured using the irradiance of an Osram HLX 64623 halogen bulb (color temperature = 3200 K) as standard.

References

1 Lewis, N. S. & Nocera, D. G. Powering the planet: Chemical challenges in solar energy utilization. *Proc. Natl. Acad. Sci. USA* **103**, 15729-15735 (2006).

2 Bard, A. J. & Fox, M. A. Artificial photosynthesis: Solar splitting of water to hydrogen and oxygen. *Acc. Chem. Res.* **28**, 141-145 (1995).

3 Walter, M. G. *et al.* Solar water splitting cells. *Chem. Rev.* **110**, 6446-6473 (2010).

4 Li, Z. S., Luo, W. J., Zhang, M. L., Feng, J. Y. & Zou, Z. G. Photoelectrochemical cells for solar hydrogen production: current state of promising photoelectrodes, methods to improve their properties, and outlook. *Energ. Environ. Sci.* **6**, 347-370 (2013).

5 Aharon-Shalom, E. & Heller, A. Efficient p-InP (Rh-H alloy) and p-InP (Re-H alloy) hydrogen evolving photocathodes. *J. Electrochem. Soc.* **129**, 2865-2866 (1982).

6 Boettcher, S. W. *et al.* Photoelectrochemical hydrogen evolution using Si microwire arrays. *J. Am. Chem. Soc.* **133**, 1216-1219 (2011).

7 Khaselev, O. & Turner, J. A. A monolithic photovoltaic-photoelectrochemical device for hydrogen production via water splitting. *Science* **280**, 425-427 (1998).

8 Seger, B. *et al.* Using TiO_2 as a conductive protective layer for photocathodic H_2 evolution. *J. Am. Chem. Soc.* **135**, 1057-1064 (2013).

9 McKone, J. R., Pieterick, A. P., Gray, H. B. & Lewis, N. S. Hydrogen evolution from Pt/Ru-coated *p*-type WSe_2 photocathodes. *J. Am. Chem. Soc.* **135**, 223-231 (2012).

10 Paracchino, A., Laporte, V., Sivula, K., Gratzel, M. & Thimsen, E. Highly active oxide photocathode for photoelectrochemical water reduction. *Nat. Mater.* **10**, 456-461 (2011).

11 Hou, Y. D. *et al.* Bioinspired molecular co-catalysts bonded to a silicon photocathode for solar hydrogen evolution. *Nat. Mater.* **10**, 434-438 (2011).

12 Warren, E. L., McKone, J. R., Atwater, H. A., Gray, H. B. & Lewis, N. S. Hydrogen-evolution characteristics of Ni-Mo-coated, radial junction, n^+p-silicon microwire array photocathodes. *Energ. Environ. Sci.* **5**, 9653-9661 (2012).

13 Seger, B. *et al.* Hydrogen production using a molybdenum sulfide catalyst on a titanium-protected n^+p-Silicon Photocathode. *Angew. Chem. Int. Ed.* **51**, 9128-9131 (2012).

14 Zhang, Z. *et al.* Carbon-layer-protected cuprous oxide nanowire arrays for efficient water reduction. *ACS Nano* **7**, 1709-1717 (2013).

15 Bourgeteau, T. *et al.* A H_2-evolving photocathode based on direct sensitization of MoS_3 with an organic photovoltaic cell. *Energ. Environ. Sci.* **6**, 2706-2713 (2013).

16 Lin, C.-Y., Lai, Y.-H., Mersch, D. & Reisner, E. $Cu_2O|NiO_x$ nanocomposite as an inexpensive photocathode in photoelectrochemical water splitting. *Chem. Sci.* **3**, 3482-3487 (2012).

17 Laursen, A. B. *et al.* MoS_2-an integrated protective and active layer on n^+p-Si for solar H_2 evolution. *Phys. Chem. Chem. Phys.* **15**, 20000-2004 (2013).
18 Merki, D., Fierro, S., Vrubel, H. & Hu, X. L. Amorphous molybdenum sulfide films as catalysts for electrochemical hydrogen production in water. *Chem. Sci.* **2**, 1262-1267 (2011).
19 Vrubel, H., Merki, D. & Hu, X. Hydrogen evolution catalyzed by MoS_3 and MoS_2 particles. *Energ. Environ. Sci.* **5**, 6136-6144 (2012).
20 Vrubel, H. & Hu, X. Growth and activation of an amorphous molybdenum sulfide hydrogen evolving catalyst. *ACS catal.* **3**, 2002-2011 (2013).
21 Prévot, M. S. & Sivula, K. Photoelectrochemical Tandem Cells for Solar Water Splitting. *J. Phys. Chem. C* **117**, 17879-17893 (2013).
22 Paracchino, A. *et al.* Ultrathin films on copper(I) oxide water splitting photocathodes: a study on performance and stability. *Energ. Environ. Sci.* **5**, 8673-8681 (2012).
23 Tilley, S. D., Schreier, M., Azevedo, J., Stefik, M. & Graetzel, M. Ruthenium oxide hydrogen evolution catalysis on composite cuprous oxide water-splitting photocathodes. *Adv. Funct. Mater.*, doi:10.1002/adfm.201301106 (2013).
24 Paracchino, A., Brauer, J. C., Moser, J. E., Thimsen, E. & Graetzel, M. Synthesis and characterization of high-photoactivity electrodeposited Cu_2O solar absorber by photoelectrochemistry and ultrafast spectroscopy. *J. Phys. Chem. C* **116**, 7341-7350 (2012).
25 Vrubel, H. & Hu, X. Molybdenum boride and carbide catalyze hydrogen evolution in both acidic and basic solutions. *Angew. Chem. Int. Ed.* **51**, 12703-12706 (2012).

Acknowledgements

This work is supported by a European Research Council (ERC) starting grant (no.257096) to X.L. Hu. S.D.T. and M.G. thank the Swiss Federal Office for Energy (PECHouse Competence Center, contract number SI/500090–02) for financial support. We thank the Interdisciplinary Centre for Electron Microscopy CIME at EPFL for their help in SEM and XPS measurements.

Author contributions

C.G.M-G. and S.D.T fabricated the electrodes. C.G.M-G. conducted the SEM and XPS experiments. C.G.M-G. and H.V. carried out the PEC experiments. All authors analyzed the data. X.L.H. and M.G. conceived the project and supervised the research work. C.G.M-G and X.L.Hu wrote the paper, with inputs from S.D.T., H.V., and M.G.

Additional information

Supplementary Information accompanies this paper at

http://www.nature.com/naturecommunications.

Competing financial interests: The authors declare no competing financial interests.

Figure Legends

Figure 1| MoS_{2+x}-Cu_2O photocathode. (a) Schematic structure of the surface-protected photocathode showing photon absorption and generation of an electron-hole pair in the *p*-Cu_2O. The extraction of the excited electron through the TiO_2 protective layers to produce hydrogen on the MoS_{2+x} catalyst is also illustrated. **(b)** A digital image of a MoS_{2+x}-CA-Cu_2O photocathode. Scale bar corresponds to 5 mm. The area covered with the MoS_{2+x} catalyst (66 μg cm^{-2}) is in the middle of the photoelectrode and corresponds here to 0.48 cm^2.

Figure 2| SEM images of thin film Cu_2O photocathodes. (a) Surface-protected photocathode before HER catalyst deposition. Scale bar corresponds to 1 μm. **(b)** Photocathode after MoS_{2+x} catalyst photo-electrochemical deposition by cyclic voltammetry (CV) and activation for H_2 evolution for 1 h at pH 1.0. Scale bar corresponds to 1 μm. **(c)** (left) Cross-sectional SEM image of the protective layers (20 nm AZO and 100 nm TiO_2) on Cu_2O and (right) a ca. 100 nm of MoS_{2+x} film on top of the protected Cu_2O electrode. Scale bars correspond to 200 nm.

Figure 3| Solar driven PEC hydrogen evolution. Current-potential curves at different pH values for a MoS_{2+x}-CV-Cu_2O photocathode (10^{th} scan). Scan rate is 10 mV s^{-1} in the cathodic direction. The geometric surface area is 0.3 cm^2 and the catalyst loading is 30 μg cm^{-2}.

Figure 4| Long-term stability and Faradaic efficiency of the MoS_{2+x}-coated Cu_2O photocathode. (a) Photocathode stability at 0 V vs. RHE for Cu_2O photocathodes modified by different HER catalysts under constant AM 1.5 illumination. **(b)** Calculated vs. real hydrogen production using a MoS_{2+x}-CA-Cu_2O photocathode (biased at 0V vs. RHE) under chopped AM 1.5 irradiation at pH 4.0. The theoretical and experimental values represent the expected and observed amount of H_2 produced, assuming a quantitative Faradaic yield for H_2 formation after an activation process of 20 min.

Figure 5| Band energy diagram. Band energy positions for the Cu_2O photocathode with Al-doped ZnO (AZO) and TiO_2 overlayers and the MoS_{2+x} catalyst film biased at 0 V vs. RHE in the dark assuming pinning of the band edges of the semiconductor at the interfaces.

Figures

Figure 1a.

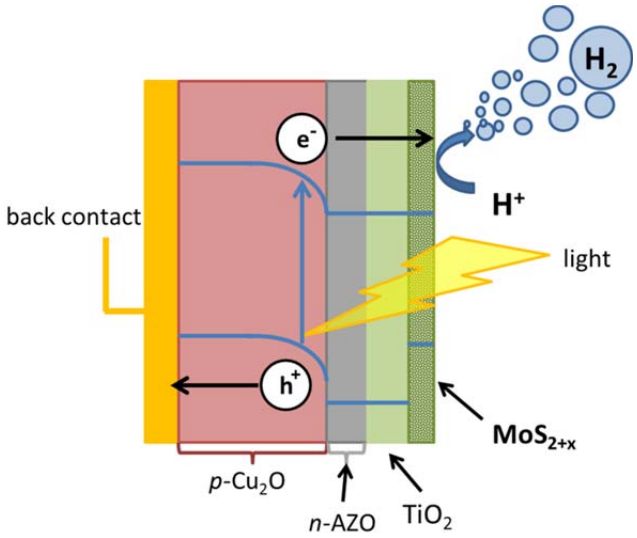

Figure 1b.

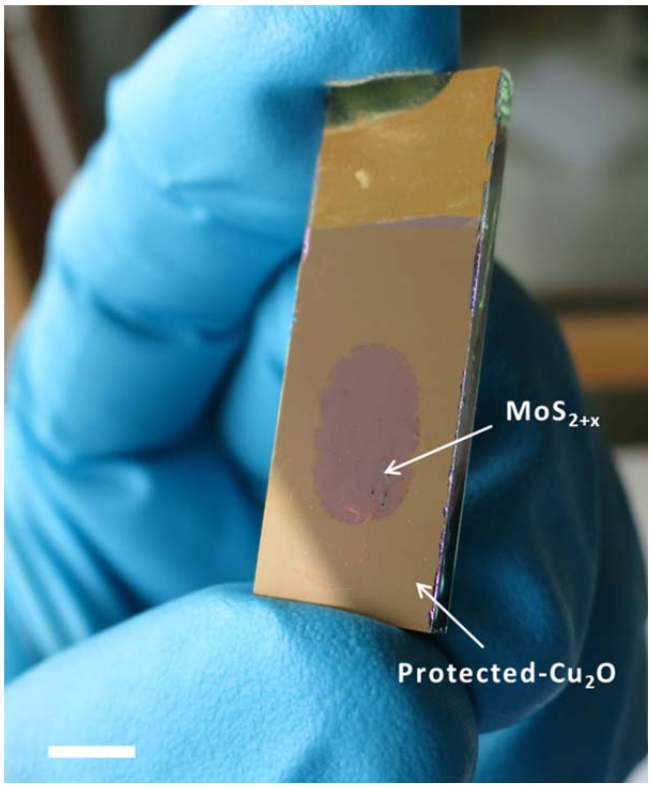

Figure 2a.

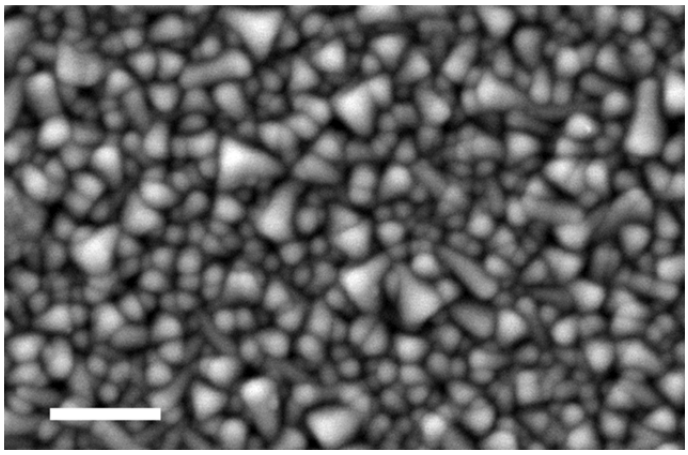

Figure 2b.

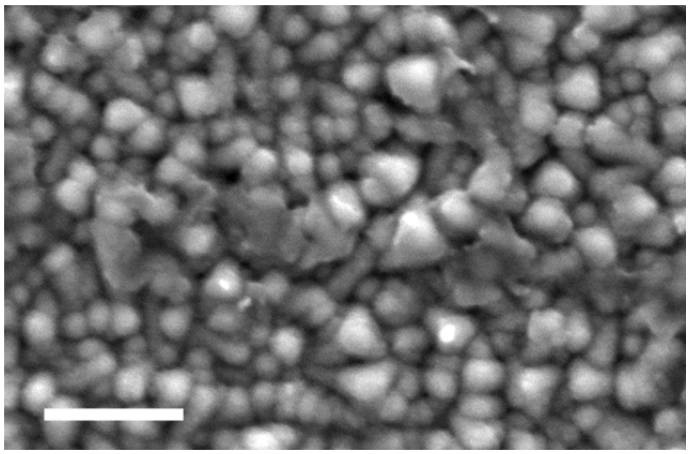

Figure 2c.

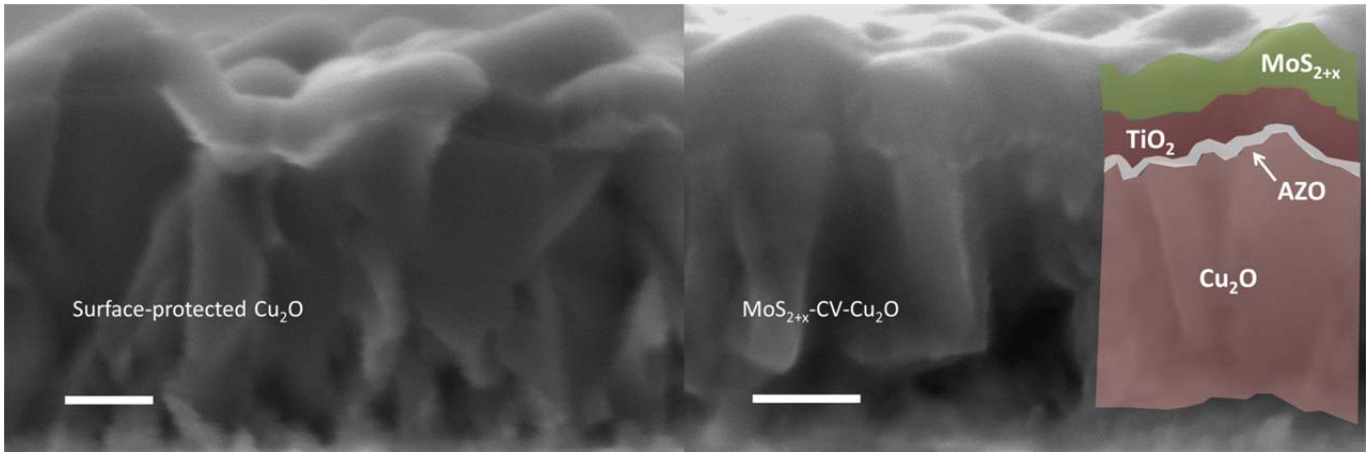

Figure 3.

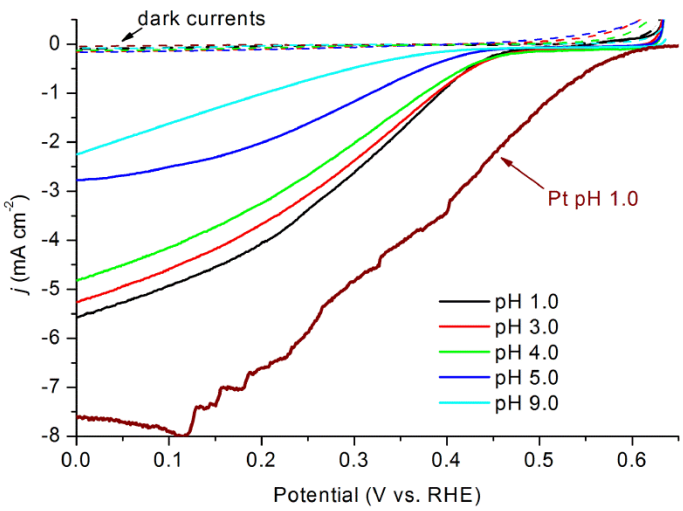
dark currents
Pt pH 1.0
pH 1.0
pH 3.0
pH 4.0
pH 5.0
pH 9.0
j (mA cm-2)
Potential (V vs. RHE)
0
-1
-2
-3
-4
-5
-6
-7
-8
0.0
0.1
0.2
0.3
0.4
0.5
0.6

Figure 4a.

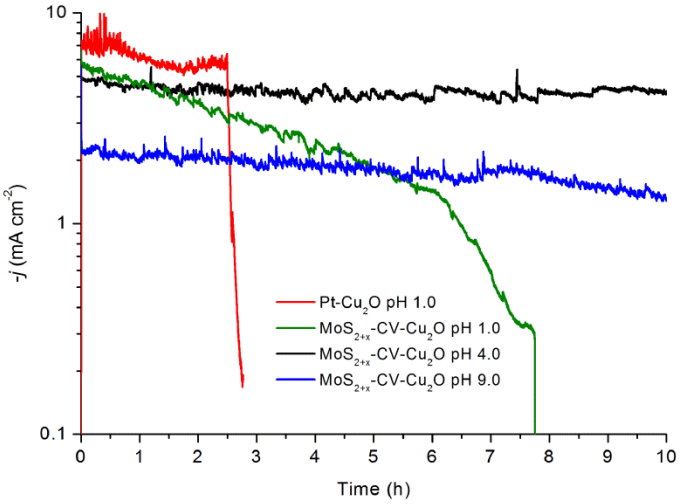

Figure 4b.

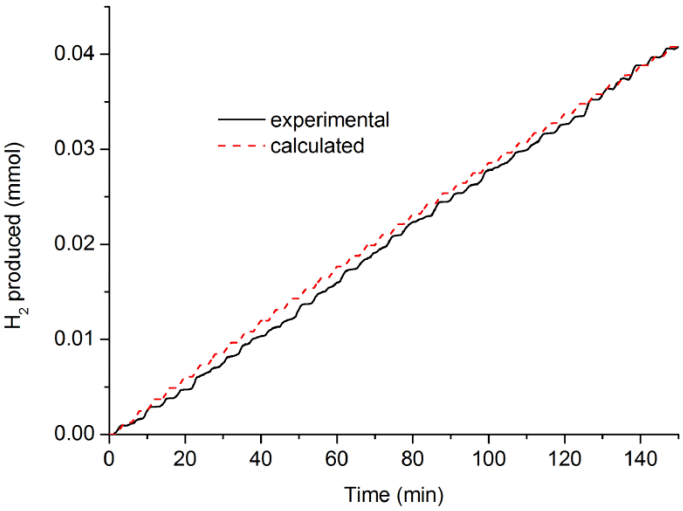

Figure 5.

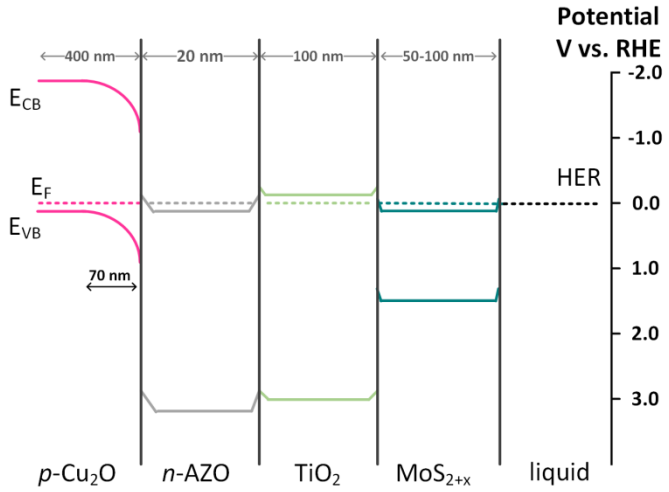

Thumbnail figure